High-Stability Quantum Dot-Converted 3-in-1 Full-Color Mini-Light-Emitting Diodes Passivated With Low-Temperature Atomic Layer Deposition

Yu-Ming Huang, Tanveer Ahmed, An-Chen Liu, Sung-Wen Huang Chen, Kai-Ling Liang, Yu-Hau Liou, Chao-Cheng Ting, Wei-Hung Kuo, Yen-Hsiang Fang, Chien-Chung Lin, *Senior Member, IEEE*, and Hao-Chung Kuo, *Fellow, IEEE*

***Abstract*— In this study, we demonstrate a 3-in-1 mini-light emitting diodes (LEDs) with 160 × 65 μm^2 mini-LED subpixel chip size. Blue mini-LEDs are combining with red and green quantum dots (QDs) by using ink-jet printing technique to achieve a full-color and high-quality mini-LEDs array in the form of a monolithic chip. Subsequently, low-temperature passivated by atomic layer deposition (ALD) at 50 °C is used to effectively avoid the photo-oxidation and maintain the color purity, 99.5% National Television Standards Committee (NTSC) and 89.6% of Rec. 2020 color gamut of red as well as green QDs (GQDs) during 300 h reliability test under 50 °C/50% relative humidity (RH) condition. The environment stability L50 of both samples is 6761 and 5889 h for red and green QDs. Finally, we advocate the potential of the demonstrated highly stable full-color QD mini-LEDs to be applied in the display technology. This research also meets the requirement for a simple QD deposition method which is expected to achieve a breakthrough.**

Manuscript received September 19, 2020; revised November 28, 2020; accepted December 15, 2020. Date of publication January 13, 2021; date of current version January 22, 2021. This work was supported by the Ministry of Science and Technology, Taiwan (107-2221-E-009-113-MY3, 108-2221-E-009-113-MY3, 109-2124-M-009-010-). The review of this article was arranged by Editor C. Bayram. *(Yu-Ming Huang and Tanveer Ahmed contributed equally to this work.) (Corresponding author: Hao-Chung Kuo.)*

Yu-Ming Huang and Chein-Chung Lin are with the College of Photonics, Institute of Photonic System, National Chiao Tung University, Tainan 71150, Taiwan (e-mail: michael_4212.05g@g2.nctu.edu.tw; chienchunglin@faculty.nctu.edu.tw).

Tanveer Ahmed is with the Department of Electrical Engineering and Computer Engineering, National Chiao Tung University, Hsinchu 30010, Taiwan (e-mail: tahmed949@gmail.com).

An-Chen Liu, Sung-Wen Huang Chen, Yu-Hau Liou, Chao-Cheng Ting, and Hao-Chung Kuo are with the Department of Photonics, National Chiao Tung University, Hsinchu 30010, Taiwan, and also with the College of Electrical and Computer Engineering, Graduate Institute of Electro-Optical Engineering, National Chiao Tung University, Hsinchu 30010, Taiwan (e-mail: arsen.liou@gmail.com; wenisbest.nctu@gmail.com; randyliouyuhau@gmail.com; chaochengting.mse00g@g2.nctu.edu.tw; hckuo@faculty.nctu.edu.tw).

Kai-Ling Liang, Wei-Hung Kuo, and Yen-Hsiang Fang are with the Electronic and Optoelectronic System Research Laboratories, Industrial Technology Research Institute, Hsinchu 31040, Taiwan (e-mail: kl@itri.org.tw; guoweihong@itri.org.tw; yhfang@itri.org.tw).

Color versions of one or more figures in this article are available at https://doi.org/10.1109/TED.2020.3048640.

Digital Object Identifier 10.1109/TED.2020.3048640

***Index Terms*— Full-color, light-emitting diodes (LEDs), low-temperature atomic layer deposition (ALD), quantum dots (QDs), reliability.**

I. Introduction

THE quantum dots (QDs) are nanosized luminescent materials with a range of applications in modern-day technologies. QDs (also termed as semiconductor nanocrystals) exhibit unique electronic and optical properties that differ from the properties of bulk semiconductor materials. QDs have discrete electronic states, similar to those of natural atoms, and their electronic wave function is somewhat analogous to that of a real atom. Therefore, they are frequently termed artificial atoms [1], [2]. QDs are used in a diverse range of technologies, such as solar cells [3]–[5], photodetectors [6], photocrystals [7], field-effect transistors [8], biological systems [9], [10], and light-emitting diodes (LEDs) [11]–[14].

The use of QDs in optoelectronic devices is increasingly popular because QDs are convenient for incorporation into optoelectronic devices of various types and sizes. One of the numerous applications of QDs in optoelectronic devices is their use as an alternative to conventional phosphor materials in LEDs. Optically pumped QD-LEDs have been demonstrated to suit both general lighting and display applications and reduce the difficulty of the mass-transfer process [15], [16]. The motivation to use QDs as color-converting substances originates from the exciting advantages that this technique offers, such as saturated colors, tunable emissions, ultrasmall grain sizes, solution-based workability, and high luminescent efficiency. QDs can be combined with macro-sized LEDs to produce general lighting devices, whereas their use with mini-LEDs and micro-LEDs can create display backlight units and high-resolution self-emissive displays, respectively [17], [18]. Solution-processed QDs can be printed on LEDs of various sizes by using several techniques such as spin coating [19] and ink-jet printing [20]. Aerosol Jet printing and Super Inkjet (SIJ) printing have been reported to yield fine pitch printing of QDs, which is a crucial requirement for achieving full-color QD-converted micro-LEDs with high resolutions [21].

0018-9383 © 2021 IEEE. Personal use is permitted, but republication/redistribution requires IEEE permission.
See https://www.ieee.org/publications/rights/index.html for more information.

Authorized licensed use limited to: Conestoga College. Downloaded on February 27,2021 at 02:04:22 UTC from IEEE Xplore. Restrictions apply.

A critical concern regarding QDs is their stability against temperature and exposure to light. QDs pumped with electrically driven LEDs usually display photoluminescence (PL) decay caused by oxidative and thermal deterioration. This type of PL decay becomes more severe at elevated operating current values for LEDs being used as a pumping source for QDs because higher currents correspond to enhanced heating effects. Many approaches to overcoming this concern have been proposed in the literature. The potential solutions include a multicore QD structure [22], liquid-type packaging [23], and use of a passivating thin film. The deposition of a passivating layer by using a thin-film deposition technique, such as atomic layer deposition (ALD), is effective in avoiding PL decay of QDs [24]–[26] because passivating films minimize the oxidation phenomenon by removing reactive sites on the QD layer and makes QDs resistant to heat-induced deterioration. In this article, we report a 3-in-1 mini-LED with a chip size of $160 \times 65\ \mu m^2$. Printing facility named SIJ printer is purchased from SIJ Technology, Inc., and the product number is SIJ-S050. SIJ provides high-quality submicrometer scale printing profiles with narrow linewidth, which helps meeting the requirement of high resolution. In order to enhance the color conversion efficiency, we fabricated 35-μm black photoresist (PR) matrices in order to confine the thick QD layer. Moreover, the usage of low-temperature ALD technology can effectively avoid oxidation and moisture, furtherly, maintains the color purity of red and green. As conventional ALD reactors usually require high temperatures to operate, there is always a collateral damage caused by the in-process heating. Due to low-temperature ($<$50 °C) ALD passivation process, we make sure that process-induced heating issues are well-prevented which could make QDs degrade [27], [28]. Moreover, ALD passivation films are usually low-stressed and amorphous, which would be improved mechanical stability and reliability by the reduction or removal of crystalline grain boundaries and surface layer defects [29].

II. Experiment

A highly stable QDs-integrated mini-LEDs array with full-color emission capability was developed in this study. First, a blue mini-LEDs array was developed, on which red and green QDs could be deposited to achieve a full-color display. Epitaxial wafers comprising multiple quantum well structures were used. The active layer was composed of InGaN/GaN multiple quantum wells. The other layers included an undoped GaN buffer layer, a p-type GaN layer, and an n-type GaN layer. The cumulative thickness of all the layers, grown on a sapphire substrate, was 7 μm. The device fabrication process consisted of two main parts. First, a mini-LEDs array with blue emission was prepared and the area of each subpixel of mini-LEDs was $160 \times 65\ \mu m^2$, as illustrated in Fig. 1(a). Second, a black PR matrix with a $140 \times 40\ \mu m^2$ window was deposited and red and green QDs were then printed to produce red, green, and blue (RGB) pixels.

At the beginning of the mini-LEDs process, a distributed Bragg reflector (DBR) was deposited at the top of the LED epitaxial structure. The selective area etching of PR and LED

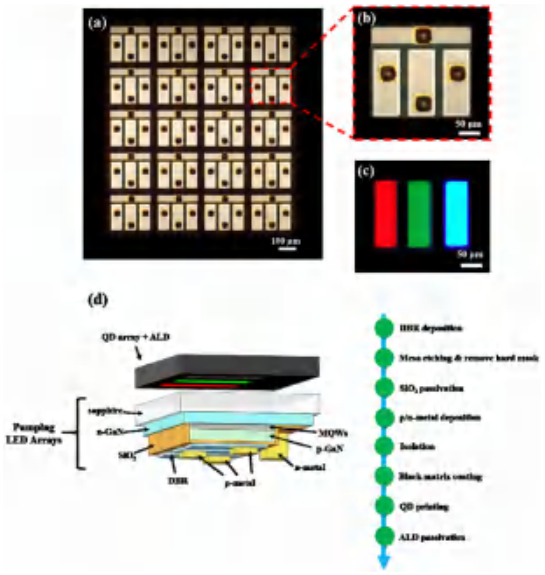

Fig. 1. Optical microscope image of (a) 3-in-1 mini-LEDs array, (b) single pixel of the mini-LEDs array, (c) EL microscope image of RGB pixel, and (d) process flow and the schematic of full-color 3-in-1 mini-LEDs device.

layers was followed by the use of an inductively coupled plasma reactive ion etching (ICP-RIE) machine. A layer of SiN_x was then deposited using plasma-enhanced chemical vapor deposition (PECVD), which was then used for selective SiN_x through-hole etching. Lithographic techniques were used for patterning, and ICP-RIE was used for etching SiN_x using a method that enables the deposition of both p-metal and n-metal contacts by the electron beam evaporation. The composition of the contact material was Ti/Pt/Au. The final step of the mini-LEDs process was the deposition of the black matrix (BM) PR materials with a thickness of approximately 35 μm out of the sapphire side. Both the materials were deposited during the lithography process. Color filters were then fabricated by printing thin layers of red and green QDs in the BM by SIJ system. The red and green QD inks comprised CdSe/ZnS core-shell QDs dissolved in toluene, which have 90% and 95% photoluminescence quantum efficiency, concentrations are 10 and 5 mg/mL as phosphor material. Moreover, for the parameters of SIJ system, the print speed is 0.2 mm/s, dc voltage is 256 V, and Eject wait time is 60–80 ms. In order to optimize the photoluminescent quantum yield (PLQY) of QDs, we repeatedly printing into the 35 μm to increase the thickness of QDs. A matrix containing pixels emitting all three primary colors was finally achieved, it efficiently solved the mass-transfer issue. Fig. 1(b) shows a single-pixel mini-LEDs array and Fig. 1(c) is the electroluminescence (EL) microscope image of RGB pixel. Finally, a thermal ALD process of 75-nm Al_2O_3 protective layer (deposition rate is 0.1 Å/s) was deposited on the RGB pixel through 50 °C low-temperature ALD passivation, which is using trimethylaluminum ($Al(CH_3)_3$, TMA) as a precursor and water as a coreactant. Due to the low-temperature property, it not only prevented the QDs from photo-oxidation and photo-corrosion [29] but reduced the power consumption for ALD passivation equipment. The whole process for 3-in-1 mini-LEDs and schematic are as shown in Fig. 1(d).

Authorized licensed use limited to: Conestoga College. Downloaded on February 27,2021 at 02:04:22 UTC from IEEE Xplore. Restrictions apply.

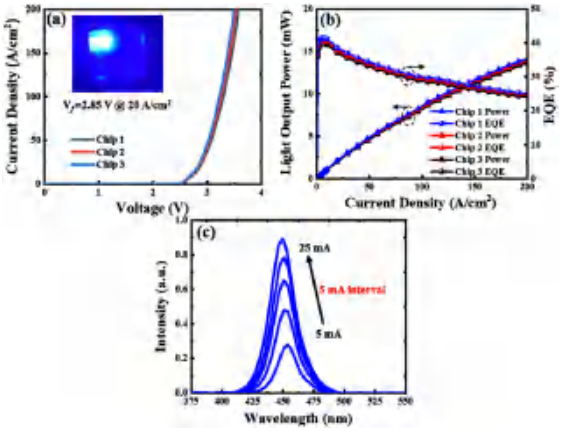

Fig. 2. (a) *J–V* curve of 3-in-1 mini-LEDs, with an image of the lighting from the device. (b) Light output power and EQE of 3-in-1 mini-LEDs. (c) EL spectrum of the mini-LEDs with increasing applied current density.

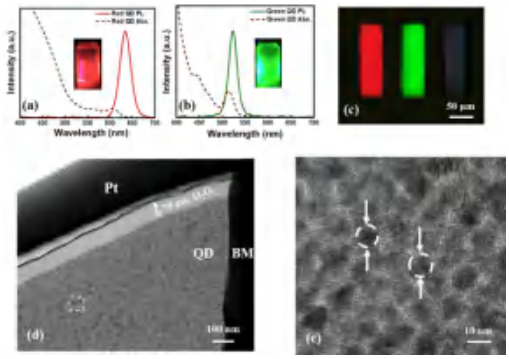

Fig. 3. (a) and (b) EL spectra and absorption of the red and green QDs, respectively. (c) Fluorescence microscopy image of RGB pixels. (d) TEM image of 75-nm Al_2O_3 deposited on QD. (e) TEM image of the green quantum dot (GQD) area.

III. Results and Discussion

The optical–electrical characteristics of mini-LEDs devices are summarized in Fig. 2. Fig. 2(a) illustrates the current density–voltage (J–V) characteristic of a 3-in-1 mini-LEDs with a subpixel size of 160 × 65 μm^2; a forward voltage of 2.85 V at 20 A/cm^2 indicates electrical properties. The output power and external quantum efficiency (EQE) are shown in Fig. 2(b), which illustrates 39.98% at 5.75 A/cm^2 of EQE value. The EL spectrum at various current conditions under 5-mA interval is illustrated in Fig. 2(c). The EL spectrum displays a 453-nm peak wavelength and 28.25 nm full width at half maximum (FWHM) under the 95 A/cm^2 driving condition. The narrow FWHM indicates the high quality of the 3-in-1 sample.

We used CdSe/ZnS-based core-shell QDs that exhibit over 90% PLQY of phosphor which were purchased from Unique Materials Co., Ltd. Fig. 3(a) and (b) shows the red and green QDs emission spectrum and absorption spectrum. The peak wavelengths were obtained at 627 and 537 nm, and the FWHMs were obtained at 28.4 and 21.6 nm, respectively. The high contrast ratio between the black matrices (BM) and color pixels obtained through inkjet printing under the fluorescence microscopy image is illustrated in Fig. 3(c).

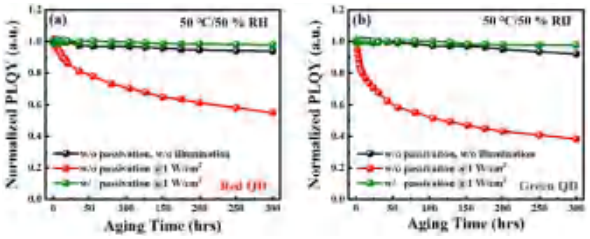

Fig. 4. PLQY of (a) RQDs and (b) GQDs on black matrices under different excitation conditions [50 °C/50% relative humidity (RH)].

The black PR mold could achieve a height of 35 μm and prevent the blue light side leakage, thereby reducing the crosstalk effect between the pixels. The transmission electron microscopy (TEM) image is demonstrated in Fig. 3(d), and we could clearly observe a 75-nm-thickness layer of Al_2O_3 deposited on the QDs uniformly. Moreover, we can also observe the morphology of QDs with diagram of approximately 5 nm in Fig. 3(e).

A reliability test for red quantum dots (RQDs) on BM samples was performed for 300 h, where one of the samples was not pumped continuously with a blue LED and the others were pumped by 1 W/cm^2 continuously reliability test. Because of their large surface-to-volume ratio and poor environmental stability, QDs usually present the risk of hazards, such as oxidation and photo-thermal degradation, which affect their luminescence, stability, and emission. Thermal degradation is a key factor that causes the deterioration of QDs over time. Electrical excitation of LEDs causes heating effects, such as high junction temperatures. These heating effects increase with increasing driving current. Intuitively, the performance of QDs should be affected by increasing the driving current being used as the excitation source for LEDs. We compared the performance of RQDs under different pumping conditions to illustrate how an increase in driving current causes the rapid decay of QDs over time.

Fig. 4(a) presents a comparison of the PLQY of samples of RQDs on BM under different pumping conditions. The PLQY of samples without pumping remained stable, as expected. The PLQY, defined as the ratio between the emitted and absorbed photons, is a valuable metric in assessing the performance of an optically pumped luminescent device. The PLQY of the sample excited at 1 W/cm^2 (or 60 mA) decreased rapidly over time, and a decline of almost 45% in PLQY was observed after 300 h because of thermal effects [27]. Moreover, various approaches to addressing the problem of thermal and oxidative degradation have been proposed in the literature, such as multiple-shell structuring of QDs [24], ALD [26], liquid-type packaging, and mixing of QDs with a suitable substance like silicone for enhanced stability [30]. The deposition of a passivating material layer by using thin-film deposition techniques, such as ALD passivation, can effectively fill up surface oxidation states and thus avoid oxidation-induced degradation of QDs [31]. The RQDs on the BM sample which was passivated by a 75 nm layer of Al_2O_3 preserved the original PLQY with less than a 5% decrease after 300 h. This finding indicates that the Al_2O_3 layer minimizes the

Authorized licensed use limited to: Conestoga College. Downloaded on February 27,2021 at 02:04:22 UTC from IEEE Xplore. Restrictions apply.

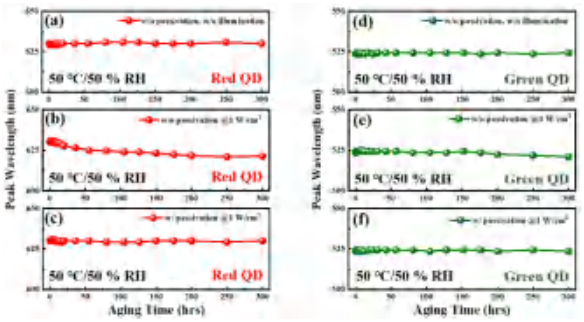

Fig. 5. Peak wavelength of (a)–(c) red QDs and (d)–(f) green QDs on black matrices under different excitation conditions (50 °C/50% RH).

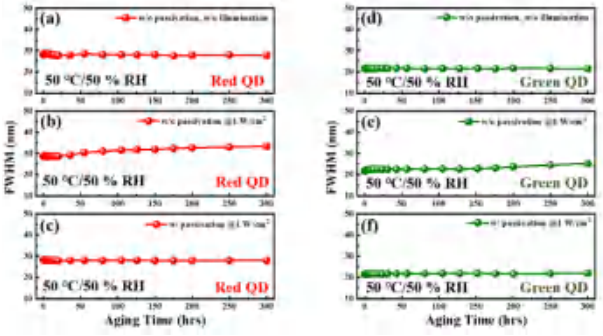

Fig. 6. FWHM of (a)–(c) red QDs and (d)–(f) green QDs on black matrices under different excitation conditions (50 °C/50% RH).

degradation caused by thermal and oxidative effects and effectively stabilizes the performance of QDs. Fig. 4(b) presents the PLQY curves of the GQDs on BM samples under three of the aforementioned conditions. Nonpassivated samples with continuous blue pumping exhibited a reduction in PLQY of approximately 60% after 300 h, whereas the other two samples did not undergo a PLQY decline over time. Green QDs are inherently known to be less efficient and less stable in comparison with their red counterparts. A reiteration of this phenomenon is observed in our experiment too as PLQY of GQDs degrades more rapidly as compared to red QDs.

QD emissions strictly depend on their size, and the peak shift in pumped RQD and GQD on BM samples indicated that excitation with blue light slightly altered the size of RQDs. All unilluminated samples displayed a stable peak wavelength, as shown in Fig. 5(a) and (d). Moreover, the nonpassivated RQD sample at 1 W/cm^2 illumination underwent an undesirable peak wavelength shift of approximately 8 nm because of thermal effects that caused loss of ligands and ultimately altered the size of QDs [32]. The GQD without ALD passivation demonstrated a 3-nm blue shift at 1 W/cm^2, as shown in Fig. 5(b) and (e). To avoid the oxidation-induced degradation of QDs, the 75-nm ALD passivation process was followed, which lead to a reduction in degradation after a 300 h burn-in test, as illustrated in Fig. 5(c) and (f). The relationship between illumination and peak wavelength contributed to the grain size of QDs [32]. During the illumination, the surface bonding ligands were easily removed resulting from photon absorption. Further, the QDs tend to be aggregated, because of the strong van der Waals force. Thus, the surface decomposition and increased trap state are critical factors for the loss of PL, which becomes more severe under high power illumination.

A narrow FWHM is desirable because it corresponds to pure and saturated color emission. The FWHMs of the samples investigated are displayed in Fig. 6. Stable FWHM values were exhibited by RQD and GQD on BM samples under no pumping conditions, as illustrated in Fig. 6(a) and (d). We also observed a stable trend in the 75-nm ALD passivation. This result suggests that ALD passivation helped maintain the spectral purity and color saturation of RQDs by preventing excitation-induced spectral broadening, as illustrated in Fig. 5(c) and (f). The RQD and GQD samples with pumping at 1 W/cm^2 displayed increases of approximately 5 and 4 nm in FWHM, respectively, after 300 h of continuous pumping,

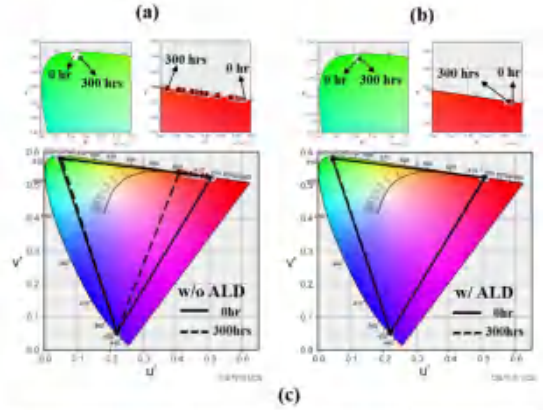

Proportion of Overlap Area	NTSC	Rec. 2020
w/o ALD passivation - 0 hr	99.6%	90.2%
w/o ALD passivation - 300 hrs	94.6%	73.5%
w/ ALD passivation - 0 hr	99.6%	90.2%
w/ ALD passivation - 300 hrs	99.5%	89.6%

Fig. 7. Color gamut of RGB pixel assembly from (a) without ALD passivation, (b) with ALD passivation at different aging times in the CIE-1976, and (c) color gamut comparison of with and without ALD passivation.

which indicated that pumping at significantly large operating currents affected the color purity of RQDs because of heat-induced degradation, as illustrated in Fig. 6(b) and (e).

Fig. 7 presents the color performance of RGB mini-LEDs with and without ALD passivation after the 0–300 h lifetime test in the International Commission on Illumination-1976 (Commission Internationale de l'éclairage) (CIE-1976). The color coordinates in the sample with no ALD passivation varied from (0.5109, 0.5239) to (0.4092, 0.5353) and (0.0451, 0.5814) to (0.0521, 0.5793) in the CIE-1976 chromaticity diagram. The color shift ($\Delta\mu'$, $\Delta\nu'$) was (0.1017, 0.0114) for red color pixels and (0.0070, 0.0021) for green pixels in the CIE-1976. Moreover, the color coordinates for the treatment sample with ALD passivation varied from (0.5076, 0.5238) to (0.5054, 0.5241) and from (0.0442, 0.5813) to (0.0467, 0.5815), and the color shifts ($\Delta\mu'$, $\Delta\nu'$) were (0.0022, 0.0003) and (0.0025, 0.0002) in the CIE-1976, respectively, as illustrated in Fig. 7(b). A color gamut comparison of RGB pixel assembly with and without ALD passivation is presented in Fig. 7(c). The sample without ALD passivation achieved 99.6% of the National Television Standards

Authorized licensed use limited to: Conestoga College. Downloaded on February 27,2021 at 02:04:22 UTC from IEEE Xplore. Restrictions apply.

Committee (NTSC) space and 90.2% Rec. 2020 in the CIE-1976, and also significantly stable during 300 h burn-in test. However, according to the sample without ALD passivation, we can observe the NTSC space decreased from 99.6% to 94.6%, and 90.2% to 73.5% in Rec. 2020. It indicated that the full-color RGB devices assembled in this study from mini-LEDs with ALD passivation displayed excellent color stability and wide color gamut features, which are promising features for display applications.

IV. Conclusion

In summary, we reported a 3-in-1 blue mini-LEDs array fabricated by a high-quality process technology, which can efficiently reduce the times of the mass-transfer. Moreover, the QD deposition is using SIJ printing followed by fabricating 35-μm black matrix layer and which achieves RGB subpixels to attain a full-color display. Low-temperature (at <50 °C) ALD passivation layer provides a stable protection to avoid QDs from photo-oxidation and humidity. The environment stability test of red and green QDs was predicted for 6761 and 5889 h at 50 °C/50% room temperature (RT) condition under 1 W/cm^2. For the sample without ALD passivation, the color gamut shift according to NTSC and Rec. 2020 standards is from 99.6% to 94.6% and from 90.2% to 73.5% in CIE-1976, whereas the color gamut of the sample with ALD passivation is almost maintained. It can be stated confidently that the usage of ALD passivation technology provides QD materials a wide color gamut and stability which shows a good color performance of the 3-in-1 mini-LEDs display.

Acknowledgment

The authors would like to thank EXCELLENCE OPTO. INC. to discuss about mini-light emitting diode (LED) array with black photoresist (PR) technology.

References

[1] R. C. Ashoori, "Electrons in artificial atoms," *Nature*, vol. 379, no. 6564, pp. 413–419, Feb. 1996.
[2] U. Banin, Y. Cao, D. Katz, and O. Millo, "Identification of atomic-like electronic states in indium arsenide nanocrystal quantum dots," *Nature*, vol. 400, no. 6744, pp. 542–544, Aug. 1999.
[3] S.-C. Hsu, Y.-M. Huang, Y.-C. Kao, H.-C. Kuo, R.-H. Horng, and C.-C. Lin, "The analysis of dual-junction tandem solar cells enhanced by surface dispensed quantum dots," *IEEE Photon. J.*, vol. 10, no. 5, pp. 1–11, Oct. 2018.
[4] H.-V. Han *et al.*, "A highly efficient hybrid GaAs solar cell based on colloidal-quantum-dot-sensitization," *Sci. Rep.*, vol. 4, no. 1, p. 5734, May 2015.
[5] K. S. Leschkies *et al.*, "Photosensitization of ZnO nanowires with CdSe quantum dots for photovoltaic devices," *Nano Lett.*, vol. 7, no. 6, pp. 1793–1798, Jun. 2007.
[6] G. Konstantatos and E. H. Sargent, "Solution-processed quantum dot photodetectors," *Proc. IEEE*, vol. 97, no. 10, pp. 1666–1683, Oct. 2009.
[7] J. Zhao, M. A. Holmes, and F. E. Osterloh, "Quantum confinement controls photocatalysis: A free energy analysis for photocatalytic proton reduction at CdSe nanocrystals," *ACS Nano*, vol. 7, no. 5, pp. 4316–4325, May 2013.
[8] W.-K. Koh, S. R. Saudari, A. T. Fafarman, C. R. Kagan, and C. B. Murray, "Thiocyanate-capped PbS nanocubes: Ambipolar transport enables quantum dot based circuits on a flexible substrate," *Nano Lett.*, vol. 11, no. 11, pp. 4764–4767, Nov. 2011.
[9] W. R. Algar and U. J. Krull, "Quantum dots as donors in fluorescence resonance energy transfer for the bioanalysis of nucleic acids, proteins, and other biological molecules," *Anal. Bioanal. Chem.*, vol. 391, no. 5, pp. 1609–1618, Jul. 2008.
[10] M. Dahan, S. Lévi, C. Luccardini, P. Rostaing, B. Riveau, and A. Triller, "Diffusion dynamics of glycine receptors revealed by single-quantum dot tracking," *Sci.*, vol. 302, no. 5644, p. 442, 2003.
[11] S.-C. Hsu *et al.*, "Highly stable and efficient hybrid quantum dot light-emitting diodes," *IEEE Photon. J.*, vol. 7, no. 5, pp. 1–10, Oct. 2015.
[12] S.-C. Hsu *et al.*, "Fabrication of a highly stable white light-emitting diode with multiple-layer colloidal quantum dots," *IEEE J. Sel. Topics Quantum Electron.*, vol. 23, no. 5, pp. 1–9, Sep. 2017.
[13] H.-Y. Lin *et al.*, "Excellent color quality of white-light-emitting diodes by embedding quantum dots in polymers material," *IEEE J. Sel. Topics Quantum Electron.*, vol. 22, no. 1, pp. 35–41, Jan. 2016.
[14] K.-J. Chen *et al.*, "Wide-range correlated color temperature light generation from resonant cavity hybrid quantum dot light-emitting diodes," *IEEE J. Sel. Topics Quantum Electron.*, vol. 21, no. 4, pp. 23–29, Jul. 2015.
[15] S.-W. H. Chen *et al.*, "Full-color monolithic hybrid quantum dot nanoring micro light-emitting diodes with improved efficiency using atomic layer deposition and nonradiative resonant energy transfer," *Photon. Res.*, vol. 7, no. 4, pp. 416–422, Apr. 2019, doi: 10.1364/PRJ.7.000416.
[16] H.-V. Han *et al.*, "Resonant-enhanced full-color emission of quantum-dot-based micro LED display technology," *Opt. Exp.*, vol. 23, no. 25, pp. 32504–32515, 2015/12/14 2015.
[17] Y.-M. Huang *et al.*, "Advances in quantum-dot-based displays," *Nanomaterials*, vol. 10, no. 7, p. 1327, Jul. 2020.
[18] T. Wu *et al.*, "Mini-LED and micro-LED: Promising candidates for the next generation display technology," *Appl. Sci.*, vol. 8, no. 9, p. 1557, Sep. 2018.
[19] D.-M. Yeh, C.-F. Huang, Y.-C. Lu, and C. C. Yang, "White-light light-emitting device based on surface plasmon-enhanced CdSe/ZnS nanocrystal wavelength conversion on a blue/green two-color light-emitting diode," *Appl. Phys. Lett.*, vol. 92, no. 9, Mar. 2008, Art. no. 091112.
[20] H. M. Haverinen, R. A. Myllylä, and G. E. Jabbour, "Inkjet printing of light emitting quantum dots," *Appl. Phys. Lett.*, vol. 94, no. 7, Feb. 2009, Art. no. 073108.
[21] Y.-M. Huang *et al.*, "The aging study for fine pitch quantum-dot array on LEDs," in *Proc. Conf. Lasers Electro-Optics*, 2019, Paper SF2O-2, doi: 10.1364/CLEO_SI.2019.SF2O.2.
[22] E. Jang, S. Jun, H. Jang, J. Lim, B. Kim, and Y. Kim, "White-light-emitting diodes with quantum dot color converters for display backlights," *Adv. Mater.*, vol. 22, no. 28, pp. 3076–3080, May 2010.
[23] C.-W. Sher *et al.*, "A high quality liquid-type quantum dot white light-emitting diode," *Nanoscale*, vol. 8, no. 2, pp. 1117–1122, 2016.
[24] R. Ihly, J. Tolentino, Y. Liu, M. Gibbs, and M. Law, "The photothermal stability of PbS quantum dot solids," *ACS Nano*, vol. 5, no. 10, pp. 8175–8186, Oct. 2011.
[25] C. Hu *et al.*, "Air-stable short-wave infrared PbS colloidal quantum dot photoconductors passivated with Al_2O_3 atomic layer deposition," *Appl. Phys. Lett.*, vol. 105, no. 17, Oct. 2014, Art. no. 171110.
[26] K. Devloo-Casier *et al.*, "A case study of ALD encapsulation of quantum dots: Embedding supported CdSe/CdS/ZnS quantum dots in a ZnO matrix," *J. Phys. Chem. C*, vol. 120, no. 32, pp. 18039–18045, Aug. 2016.
[27] K.-J. Chen *et al.*, "The influence of the thermal effect on CdSe/ZnS quantum dots in light-emitting diodes," *J. Lightw. Technol.*, vol. 30, no. 14, pp. 2256–2261, Jul. 15, 2012.
[28] J. Y. Woo *et al.*, "Visible cathodoluminescence of quantum dot films by direct irradiation of electron beam and its materialization as a field emission device," *Opt. Exp.*, vol. 21, no. 10, pp. 12519–12526, 2013.
[29] C.-Y. Cheng and M.-H. Mao, "Photo-stability and time-resolved photoluminescence study of colloidal CdSe/ZnS quantum dots passivated in Al_2O_3 using atomic layer deposition," *J. Appl. Phys.*, vol. 120, no. 8, Aug. 2016, Art. no. 083103.
[30] C.-F. Lai, Y.-C. Tien, H.-C. Tong, C.-Z. Zhong, and Y.-C. Lee, "High-performance quantum dot light-emitting diodes using chip-scale package structures with high reliability and wide color gamut for backlight displays," *RSC Adv.*, vol. 8, no. 63, pp. 35966–35972, 2018.
[31] C. Carrillo-Carrión, S. Cárdenas, B. M. Simonet, and M. Valcárcel, "Quantum dots luminescence enhancement due to illumination with UV/Vis light," *Chem. Commun.*, vol. 35, no. 35, pp. 5214–5226, 2009, doi: 10.1039/B904381K.
[32] S. Huang *et al.*, "Morphology evolution and degradation of $CsPbBr_3$ nanocrystals under blue light-emitting diode illumination," *ACS Appl. Mater. Interfaces*, vol. 9, no. 8, pp. 7249–7258, 2017.

Authorized licensed use limited to: Conestoga College. Downloaded on February 27,2021 at 02:04:22 UTC from IEEE Xplore. Restrictions apply.